Journal of ELECTRONIC MATERIALS, Vol. 44, No. 1, 2015
DOI: 10.1007/s11664-014-3365-1

Synthesis and Characterization of TiO_2 Nanotubes Sensitized with CdS Quantum Dots Using a One-Step Method

JIAHUI SONG,[1] XINGUO ZHANG,[1] CHUNYAN ZHOU,[1] YUWEI LAN,[1] QI PANG,[1] and LIYA ZHOU[1,2]

1.—School of Chemistry and Chemical Engineering, Guangxi University, Nanning 530004, China.
2.—e-mail: zhouliyatf@163.com

A novel one-step synthesis process was used to assemble CdS quantum dots (QDs) into TiO_2 nanotube arrays (TNTAs). The sensitization time of the TiO_2 nanotubes can be adjusted by controlling the CdS QD synthesis time. The absorption band of sensitized TNTAs red-shifted and broadened to the visible spectrum. The photoelectric conversion efficiency increased to 0.83%, the open-circuit voltage to 776 mV, and the short-circuit current density (J_{SC}) to 2.30 mA cm^{-2} with increased sensitization time. The conversion efficiency with this new sensitization method was five times that of nonsensitized TNTAs, providing novel ideas for study of TNTA solar cells.

Key words: Quantum dots, TiO_2 nanotube, solar cells

TNTAs have attracted significant attention in recent years as ideal photoanode materials for dye-sensitized solar cells (DSSCs). Using an anodic oxidation method to synthesize highly ordered TNTAs has several advantages, such as high energy conversion efficiency, low cost, no adverse environmental impact, and tube length stability.[1] The greatest disadvantage of TNTAs is the wide bandgap (3.2 eV), which corresponds to only around 5% solar light utilization.[2] Moreover, the energy conversion efficiency of TNTAs is limited because of the rapid recombination of photoinduced electron–hole pairs.[3] To overcome these limitations, several efforts have been made to form heterojunction structures between semiconductor QDs and TNTAs.[4–7] QDs are a type of solar cell sensitizer, arousing widespread interest because of their high extinction coefficients, multiple exciton generation effects, and tunable bandgap.[8–10] The photoelectric conversion performance of TNTAs sensitized by QDs can be improved by heightened visible light harvesting of TNTAs as the QD variety and size are concurrently adjusted.[11]

Among the most investigated QD inorganic semiconductors, CdS QDs have attracted enormous attention in QDSSC research because of their narrow bandgap (2.42 eV), which expands light absorption to the visible region.[12] Several methods to form CdS/TNTA heterojunctions have been reported, such as electrochemical deposition,[13] chemical bath deposition (CBD),[14] and successive ion layer adsorption and reaction (SILAR).[15] Although QDs are easy to combine, novel methods need to be explored to improve the photoelectric efficiency.

In this report, a new and simple method is proposed to sensitize TNTAs during a one-step CdS QD synthesis process. Figure 1 shows a schematic of the synthesis process. QD synthesis and TNTA sensitization are performed simultaneously. CdS QDs are evenly distributed on TiO_2 nanotubes because the overall reaction process is carried out under constant stirring and heating conditions. The report also provides novel ideas for researching QD-sensitized TiO_2 nanotube solar cells.

EXPERIMENTAL PROCEDURES

Preparation of TiO_2 Nanotube Arrays

High-purity titanium (0.35-mm-thick foils, 99.6% purity) was used in the experiment. Ti foils (1.0 cm × 2.0 cm) were polished mechanically, rinsed ultrasonically in acetone, ethanol, and deionized (DI) water for 15 min, and dried separately in nitrogen

(Received March 17, 2014; accepted August 1, 2014; published online September 17, 2014)

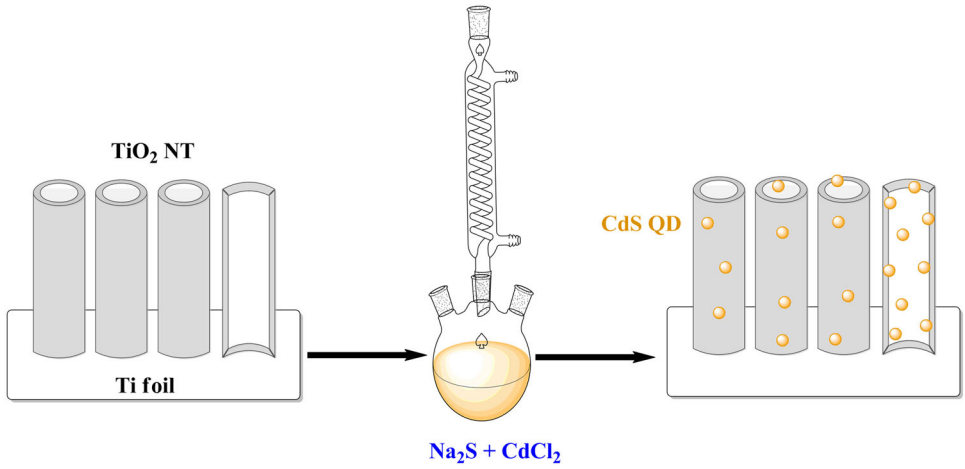

Fig. 1. Synthesis process of CdS QD-sensitized TiO_2 NTAs.

gas. Cleaned Ti foils were used as the anode, whereas a lead oxide electrode was used as the cathode for electrochemical anodization in a two-electrode cell. The distance between the two electrodes was fixed at 3.5 cm. The electrolyte was composed of deionized water and glycerol (at volume ratio of 1:5) containing NH_4F (0.5 wt.%). The two-electrode configuration was fixed to a constant voltage of 45 V for 10 h. TNTAs were cleaned with deionized water after anodization, immersed in 0.1 M HCl solution for 30 min, cleaned again with deionized water, then air-dried. These specimens were annealed at 450°C for 3 h in air with a heating rate of 1°C min^{-1} and naturally cooled down afterwards.

Fabrication of TiO_2 Nanotube Arrays Sensitized with CdS Quantum Dots

Up to 100 mL of 0.02 M $CdCl_2{\cdot}2.5H_2O$ solution was gently instilled into a 250-mL three-necked flask, then L-cysteine (0.4848 g) was stirred in. The pH value of the reaction solution was adjusted to 10.5 by stirring in 1.0 M NaOH solution. Afterward, Na_2S (0.1203 g) was added into the mixture. Annealed samples of TNTAs were loaded into the three-necked flask. The reaction was refluxed at 100°C for 0.5 h, 1 h, 2 h, and 3 h.

Characterization

X-ray powder diffraction (XRD) analysis was conducted using a Rigaku Ultima IV x-ray diffractometer. Scanning electron microscopy (SEM) images and energy-dispersive spectrometry (EDS) patterns were recorded on an FEI Quanta 200 scanning electron microscope. High-resolution transmission electron microscopy (HRTEM) images were recorded on a JEOL-2100F. Absorption spectra were measured using a TU-1901PC spectrometer. The photoelectric conversion efficiency was calculated from

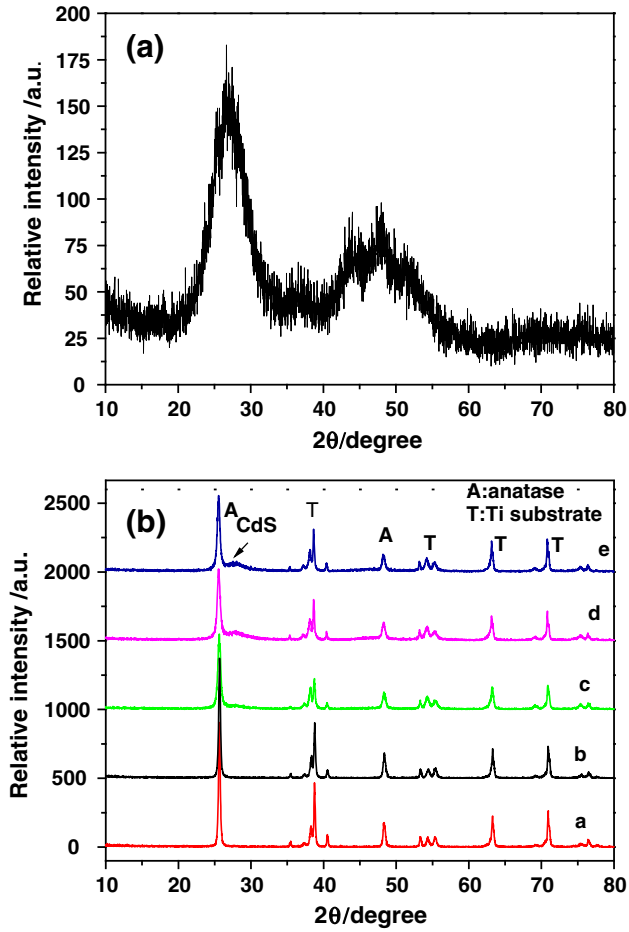

Fig. 2. XRD patterns of (A) CdS QDs, and (B) TiO_2 NTAs (a) and CdS/TiO_2 NTAs for different deposition times: 0.5 h (b), 1 h (c), 2 h (d), and 3 h (e).

the current density–voltage (J–V) characteristic, measured using an electrochemical station (model LK98BII) under 100 mW cm^{-2} irradiation by an Xe lamp (Oriel, 500 W) with a global AM1.5 filter for solar spectrum simulation. All measurements were

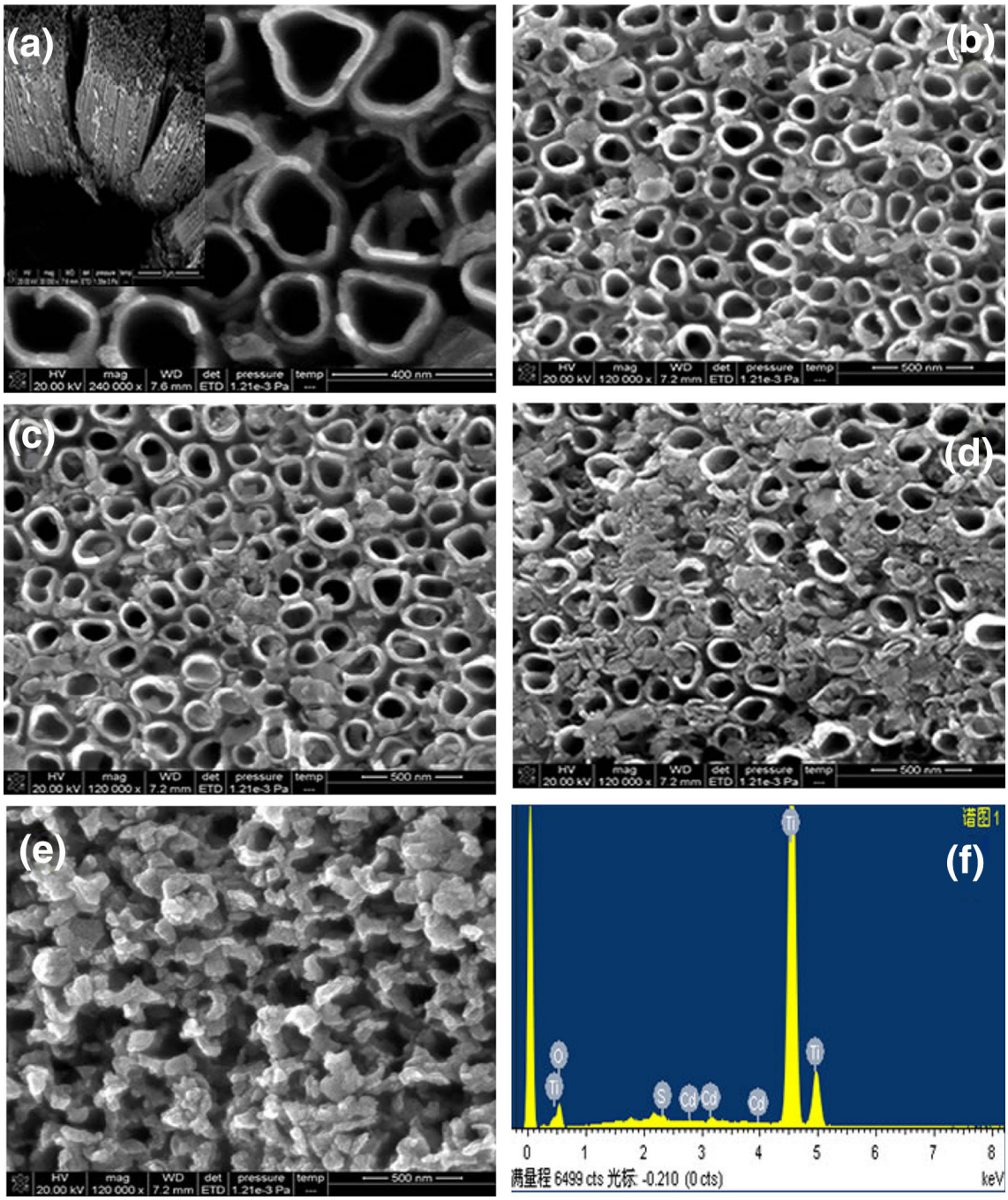

Fig. 3. (a) Top and cross-section SEM views of TiO_2 NTAs; TiO_2 NTAs sensitized with CdS for (b) 0.5 h, (c) 1 h , (d) 2 h, and (e) 3 h; (f) EDS spectrum of CdS-sensitized TiO_2 NTAs.

conducted at room temperature. In the current density–voltage (J–V) measurement process, the fill factor (FF) was calculated using Eq. 1 whereas the energy conversion efficiency (η) was calculated using Eq. 2.[16]

$$\mathrm{FF} = \frac{(J \times V)_{\max}}{J_{\mathrm{SC}} \times V_{\mathrm{OC}}}, \tag{1}$$

$$\eta = \frac{\mathrm{FF} \times \mathrm{J_{SC}} \times \mathrm{V_{OC}}}{P_{\mathrm{light}}}. \tag{2}$$

The maximum product of J and V, the short-circuit current density (J_{SC}), and the open-circuit voltage (V_{OC}) were calculated from the J–V curve; P_{light} is the incident optical power.

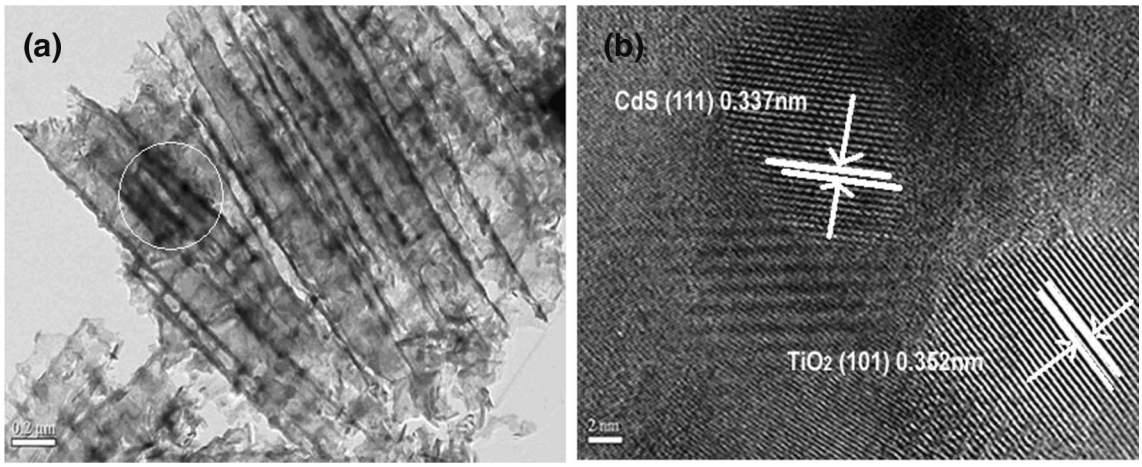

Fig. 4. HRTEM images of CdS/TiO_2 NTA heterostructures with deposition time of 2 h.

RESULTS AND DISCUSSION

XRD Characterization

Figure 2 shows the XRD patterns of CdS QDs (A) and TNTAs (B) before and after CdS QD modification. Figure 2A shows diffraction peaks at around 2θ of 26.48°, 30.68°, 43.81°, and 51.93°, which correspond to the (111), (200), (220), and (311) crystalline planes of cubic CdS [Joint Committee on Powder Diffraction Standards (JCPDS) no. 65-2887], indicating that the presence of TNTA does not affect the CdS QD synthesis. Figure 2B(a) shows the XRD pattern of TNTAs after annealing at 450°C for 3 h. XRD peak positions match those of TiO_2 anatase phase (JCPDS no. 21-1272), and the Ti peaks are in accordance with the Ti substrate. Figure 2B(b–e) shows the XRD patterns of TNTAs after being sensitized with CdS. The sensitized TNTAs have diffraction peaks missing from the pattern for the nonsensitized TNTAs. Peaks are located at −26.48°, corresponding to the CdS cubic crystalline planes (111), indicating that CdS QDs have been successfully deposited on the TNTAs and did not affect the TNTA crystal structure.

SEM, HRTEM, and EDS Characterization

Top-view and cross-section SEM images of prepared TNTAs are shown in Fig. 3a; the TNTA tube structures are shown to be uniform over a wide area. The internal tube diameter is around 160 nm, whereas the tube length ranges from 3.2 μm to 3.3 μm. The wall thickness of the TNTAs is around 30 nm. Figure 3b–e shows SEM images of TiO_2 nanotubes sensitized with CdS QDs after the reaction was refluxed at 100°C for 0.5 h (b), 1 h (c), 2 h (d), and 3 h (e). CdS QDs were successfully deposited on the TiO_2 nanotube surfaces, and the CdS QD deposition onto the TNTAs increased with prolonged sensitization time. A large number of CdS QDs almost covered the nanotube surface when the sensitization time was 3 h. Figure 3f shows the EDS spectrum of TNTAs sensitized with CdS QDs for 2 h; the obvious signals show that the nanotube arrays were composed of the elements Ti, O, Cd, and S. CdS QDs have been successfully deposited on TiO_2 nanotubes.[17]

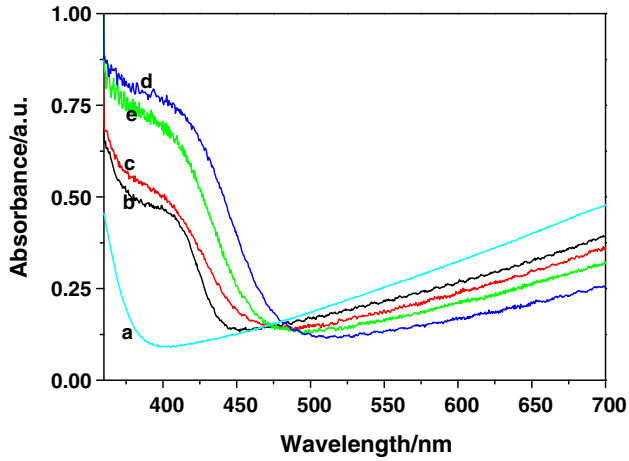

Fig. 5. UV–Vis absorption spectra of (a) TiO_2 NTAs, and CdS-sensitized TiO_2 NTAs with different deposition times: (b) 0.5 h, (c) 1 h, (d) 2 h, and (e) 3 h.

HRTEM images of the CdS/TiO_2 NTA heterostructures are shown in Fig. 4. Figure 4a shows CdS nanocrystals deposited on the inside and outside of TiO_2 TNTAs. Lattice fringes of 0.352 nm and 0.337 nm in Fig. 4b correspond to the TiO_2 anatase phase (101) plane (JCPDS no. 21-1272) and the CdS cubic (111) plane (JCPDS no. 65-2887). These results further demonstrate the formation of CdS/TiO_2 NTA heterostructures.

UV–Vis Absorption Spectroscopy

Ultraviolet–visible (UV–Vis) absorption spectra of TNTAs (a) and CdS/TNTA heterojunctions (b–e) after different reaction times are shown in Fig. 5. The maximum absorption peak edge of TiO_2 nano-

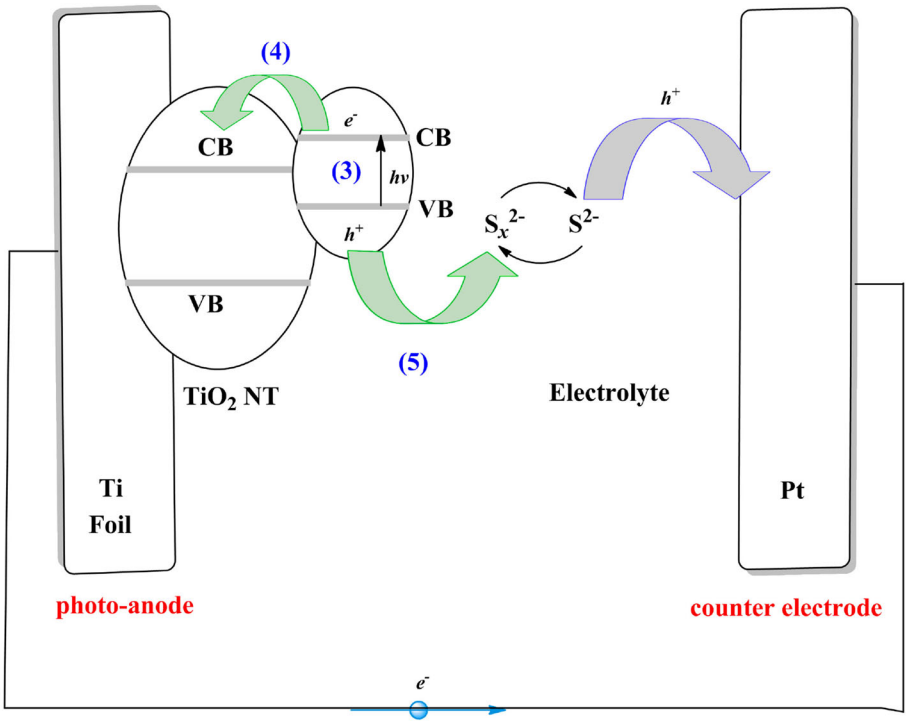

Fig. 6. Schematic illustrating CdS QD-sensitized TiO_2 nanotube solar cells.

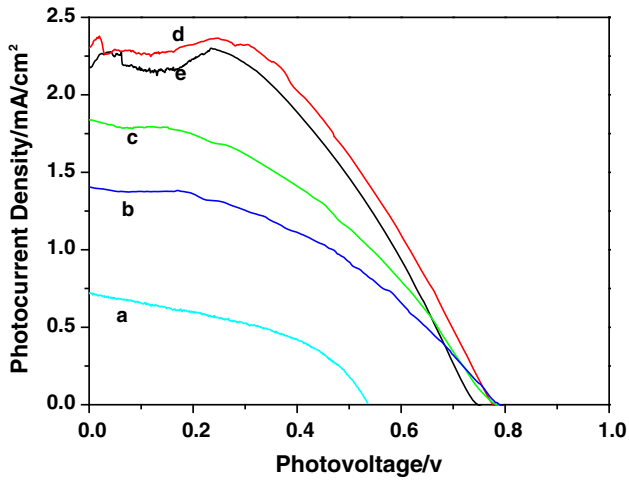

Fig. 7. Measured *J–V* characteristics for CdS/TiO_2 NTA heterostructures prepared in electrolyte: (a) TiO_2 NTAs, and with different sensitization times of 0.5 h (b), 1 h (c), 2 h (d), and 3 h (e).

tubes appears at around 380 nm, as shown in Fig. 5a. TNTAs sensitized with CdS QDs exhibited enhanced absorption and an obvious red-shift compared with pure TNTAs, indicating that TNTAs sensitized with CdS QDs have extended absorption into the visible light region.[18,19] The absorption intensity increased with prolonged reaction time, and the maximum absorption peak was at around 480 nm for 2 h of reaction time. As the reaction time was further increased beyond 2 h, the absorption intensity decreased. This quenching process is often attributed to CdS QD clustering, which reduces the TNTA surfaces exposed to visible light, leading to decreased absorption of visible light.[20]

Table I. Photovoltaic parameters of the TiO_2 and CdS/TiO_2 NTA heterostructures

Photoanode	J_{OC} (mA cm^{-2})	V_{OC} (mV)	FF	E_{ff} (%)
Bare TiO_2 nanotubes	0.73	540	0.44	0.18
CdS(0.5 h)–TiO_2 nanotubes	1.40	789	0.42	0.47
CdS(1 h)–TiO_2 nanotubes	1.84	783	0.41	0.59
CdS(2 h)–TiO_2 nanotubes	2.30	776	0.47	0.83
CdS(3 h)–TiO_2 nanotubes	2.18	747	0.46	0.76

Photovoltaic Performance of the Photoelectrodes

Photoinduced processes governing the CdS/TiO_2 photoelectrochemical behavior are depicted in Fig. 6. Electron–hole pairs are formed in the QDs when the CdS QDs are excited with visible light (Eq. 3). An electron (e^-) in the CdS QD conduction band (CB) enters the CB of the TiO_2 nanotubes (Eq. 4). Holes (h^+) are used by S^{2-} to produce polysulfide ions (S_x^{2-}) according to Eq. 5.[1,21,22]:

$$\mathrm{CdS} + h\nu \rightarrow \mathrm{CdS}\left(\mathrm{e}^- + \mathrm{h}^+\right) \quad (3)$$

$$\mathrm{CdS}\left(\mathrm{e}^- + \mathrm{h}^+\right) + \mathrm{TiO_2} \rightarrow \mathrm{CdS}\left(\mathrm{h}^+\right) + \mathrm{TiO_2}\left(\mathrm{e}^-\right) \quad (4)$$

$$\mathrm{CdS}\left(2\mathrm{h}^{+}\right) + \mathrm{S}^{2-} \rightarrow \mathrm{CdS} + \mathrm{S} \rightarrow \left(\mathrm{S}^{2-}\right) \rightarrow \mathrm{S}_{x}^{2-} \quad (5)$$

Figure 7 and Table I present the current density–voltage (J–V) curves and photovoltaic parameters of TNTAs sensitized with CdS QDs for different reaction times. The CdS QD reaction time directly affects the performance of the solar cells sensitized with QDs. The photoconversion efficiency (PCE) increases with increasing CdS QD reaction time (from 0.5 h to 2 h) and reaches its highest value of 0.83% at 2 h of reaction time. This result demonstrates that the conversion efficiency with this new sensitization method is five times that of nonsensitized TNTAs. The photoelectric conversion efficiency is 0.83%, the open-circuit voltage is 776 mV, and the short-circuit current density (J_{SC}) is 2.30 mA/cm^2. Nevertheless, J_{SC} and the PCE decreased when the CdS QD reaction time was increased to 3 h because of excess deposition of CdS QDs, causing aggregation and growth of CdS crystal nuclei, thereby inducing increased photogenerated charge-carrier recombination and decreased output.[23] Moreover, excess CdS QDs create a barrier to injection of excited electrons into TNTAs.

CONCLUSIONS

The anodic oxidation method was used to obtain highly one-dimensional ordered TNTAs. CdS QDs were assembled on TNTAs in a one-step synthesis process; the CdS QD synthesis time was controlled to tune the sensitization time. The photoelectric conversion efficiency increased to 0.83%, the open-circuit voltage to 776 mV, and the short-circuit current density (J_{SC}) to 2.30 mA/cm^2 with increased sensitization time. The conversion efficiency with a 2 h reaction time was five times that of nonsensitized TNTAs, which results in novel research ideas on TiO_2 nanotube solar cells sensitized with QDs. Moreover, our synthesis approach provides ideas for catalytic synthesis with other nanoparticles.

ACKNOWLEDGEMENTS

This work was supported by grants from the National Natural Science Foundation of China (No. 61264003).

REFERENCES

1. H.K. Jun, M.A. Careem, and A.K. Arof, *Renew. Sustain. Energy Rev.* 22, 148 (2013).
2. R. Asahi, et al., *Science* 193, 269 (2001).
3. T. Berger, et al., *J. Phys. Chem. B* 109, 6061 (2005).
4. Q. Kang, et al., *ACS Appl. Mater.* 3, 746 (2011).
5. A.C. Poulose, et al., *Chem. Phys. Lett.* 539–540, 197 (2012).
6. X.F. Gao, et al., *J. Phys. Chem. C* 113, 7531 (2009).
7. B.D.R. Baker and P.V. Kamat, *Adv. Funct. Mater.* 19, 805 (2009).
8. X.T. Ma, et al., *J. Inorg. Organomet. Polym.* 23, 798 (2013).
9. A. Kongkanand, et al., *J. Am. Ceram. Soc.* 130, 4007 (2008).
10. J.B. Sambur, T. Novel, and B.A. Parkinson, *Science* 330, 63 (2010).
11. J. Zhang, et al., *Electrochim. Acta* 83, 59 (2012).
12. S.H. Hsu, S.F. Hung, and S.H. Chien, *J. Power Sources* 233, 236 (2013).
13. S. Banerjee, et al., *Chem. Mater.* 20, 6784 (2008).
14. Y.Y. Song, et al., *Electrochem. Commun.* 16, 44 (2012).
15. X.T. Ma, et al., *J. Alloys Compd.* 538, 61 (2012).
16. Z.J. Wang, et al., *Polymer* 49, 4647 (2008).
17. J. Li, et al., *Mater. Res. Bull.* 48, 2566 (2013).
18. S.S. Kalanur, et al., *J. Photochem. Photobiol. A* 259, 1 (2013).
19. S.G. Feng, et al., *Electrochim. Acta* 83, 321 (2012).
20. J.B. Xue, et al., *Electrochim. Acta* 97, 10 (2013).
21. P.K. Santra and P.V. Kamat, *J. Am. Chem. Soc.* 134, 2508 (2012).
22. B.J.H. Bang and P.V. Kamat, *Adv. Funct. Mater.* 20, 1970 (2010).
23. H. Chen, et al., *Electrochim. Acta* 56, 919 (2010).